

Fundamentals of Ultrasonic Treatment of Aluminum Alloys

Raquel F. Jaime, Carl Söderhjelm, Diran Apelian
University of California, Irvine–Advanced Casting Research Center, Irvine, California, USA

Copyright 2024 American Foundry Society

ABSTRACT

High integrity cast aluminum (Al) components require the use of molten metal processing technologies prior to casting. These include processes such as degassing to reduce porosity, filtration to reduce inclusion content, addition of grain refiners to refine the grain structure, and the addition of chemical modifiers to alter the morphology of eutectic phases. Ultrasonic Treatment (UST) is a novel processing method through which ultrasonic energy is introduced into molten metal for the purpose of degassing as well as modifying the cast microstructure. To optimize the use and applications of UST, it is necessary to examine the fundamental mechanisms and the limiting values of controlling parameters. The mechanisms of ultrasonic energy imparted within molten metal will be discussed as well as the benefits of UST during molten metal processing.

Keywords: ultrasonic treatment, degassing, grain refinement, intermetallic morphology modification, aluminum, multi-frequency mode modulated (MMM) technology

INTRODUCTION TO ULTRASONIC TREATMENT

Aluminum (Al) alloy castings are essential in various applications where high strength, high fracture toughness, and lightweight parts are needed.^{1–5} There are multiple refinement processes and procedures that are applied to molten Al to enhance the mechanical behavior of the cast metal. Some common practices include rotary degassing, the addition of grain refiners such as TiB₂, and the addition of manganese, chromium, or other elements which can refine the morphology of intermetallic compounds. Molten metal processing technologies target inclusion content, porosity, hydrogen content, grain morphology, and intermetallic morphology. Ultrasonic treatment has shown the potential to enact changes in all these quality detractors.

Ultrasonic treatment (UST) is a processing method through which ultrasonic waves are applied to molten metal to enact microstructural change. The ultrasonic waves themselves result in physical changes within the molten metal which affect the solidification behavior, leading to changes in the microstructure.

Ultrasound is a sound wave with a frequency range of 20 kHz to 18 MHz. An ultrasonic wave is an oscillation around an equilibrium position. There are two parameters that define this motion around the equilibrium position: frequency and amplitude. Frequency is the wave period per time, or the sound wave travel from peak to peak. The amplitude is the distance vertically from the equilibrium position. Fig. 1 displays both frequency and amplitude in relation to wave shape.

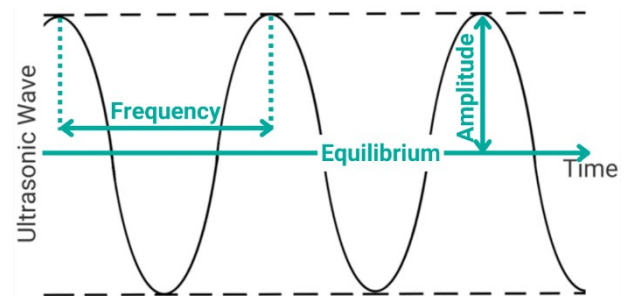


Figure 1. A visualization of a sound wave labeled with an equilibrium position, frequency, and amplitude.

Ultrasonic treatment of metal occurs within the frequency range of 18 to 22 kHz and the most crucial part of a sound wave is the amplitude. The amplitude of the wave directly relates to the intensity of the treatment applied, seen in Eqn. (1).⁶ Intensity is proportional to the square of the initial amplitude, A_0 (μm), and is also dependent on the variables c (m/s), speed of sound, ρ (kg/m^3), medium density, and ω (rad), angular frequency. The intensity of the wave is proportional to the density of the medium. Density is a measure of how closely packed atoms are within a medium and dictates the efficiency of atoms at communicating and transmitting an ultrasonic wave through the medium. Therefore, a higher density material experiences a higher intensity wave. However, increasing the density of a medium also increases the effects of loss.

$$\text{Intensity} = \frac{\text{Power}}{\text{Area}} = \frac{1}{2} \rho c (\omega A_0)^2 \quad \text{Eqn. 1}$$

An ultrasonic wave travels through a medium with a repeating unit oscillation per time, frequency, and an amplitude that oscillates equally above and below the equilibrium. This frequency and amplitude repeat indefinitely at the same magnitude in a theoretically friction-free environment. Realistically, both the frequency and amplitude decay because of losses and acoustic loading conditions in the medium. The total loss in the medium is termed attenuation. Attenuation is the

gradual loss of ultrasonic energy due to the combination of reflection, refraction, and absorption. Absorption is the sudden loss due to the wave affecting the medium and expending energy for a material response. Reflection and refraction result from the wave encountering an obstacle and are therefore less predictable than absorption. These forms of losses cause decay in both frequency and amplitude of the wave.⁶

Although both parameters experience decay, amplitude decay is what leads to decay in intensity. Ultrasonic equipment directly supplies frequency, so amplitude decay is the issue with maintaining the wave.⁶ Amplitude decay from the total loss of attenuation is shown mathematically in Eqn. (2) where A is the new decayed amplitude value, A_0 is the initial amplitude, δ is the medium constant attenuation factor, and t is the time that has passed.⁶ Amplitude decay can be found in direct relation to absorption as in Eqn. (3) where α is the medium absorption factor constant, and x is the wave path distance.⁶ It is important to note that loss and absorption occur because the wave is affecting the medium in some way. Although loss seems like a burden because it prevents the wave from traveling further into the medium. If there was no loss, then the wave would have no energy expense on the medium and therefore no effect.

$$A = A_0 e^{-\delta t} (\cos \sqrt{\omega_0^2 - \delta^2 t}) \quad \text{Eqn. 2}$$

$$A = A_0 e^{-\alpha x} \quad \text{Eqn. 3}$$

A wave traveling through the medium experiences both reflection and refraction, which causes the ultrasonic wave to be composed of both traveling and standing waves. Traveling waves are oscillations with all energy moving in one direction. Two traveling waves that move in opposite directions superimpose to produce a standing wave due to the reflection of the initial wave and equal energy in both the forward and reverse directions. Due to the movement of energy in both directions, a standing wave oscillates with double the amplitude of its equal traveling wave counterpart. This effect is visualized in Fig. 2 where two traveling waves compile to produce a larger standing wave. The traveling wave experiences attenuation and absorption throughout the medium and the standing component is produced from reflection and some refraction.

An ultrasonic wave traveling through a medium is a loaded wave and can be described in three ways; free, dampened, and forced. A free, or natural, wave is one that continues with constant frequency and constant amplitude without an external force. A dampened wave is one that experiences decay, such as attenuation and absorption, as it continues through a medium, resulting in a decrease in amplitude and frequency. A forced wave is one that experiences damping but maintains constant amplitude and frequency due to an added external force, such as an

opposing or reflecting wave that is supplementing the amplitude with the production of a standing wave. Free waves exist theoretically when there is nothing to dampen the wave or create losses. Ultrasonic waves that travel through metal melts exist as either dampened or forced.

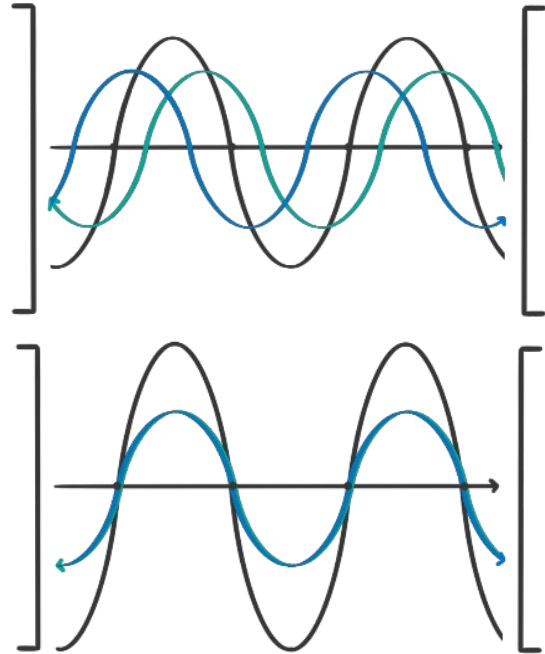


Figure 2. A blue traveling wave moving right and a green traveling wave moving left superimpose themselves, producing a gray standing wave (top), two traveling waves fully superimpose to produce a gray standing wave with double the amplitude (bottom).

PRODUCTION OF ULTRASOUND-EQUIPMENT & CONSIDERATIONS

There are four main parts involved in the production of an ultrasonic wave; an ultrasonic generator, a transducer, a wave guide, booster, and a probe. These components are further discussed.

ULTRASONIC GENERATOR

The ultrasonic generator converts electricity into voltage pulses that are required for the transducer. The controls on an ultrasonic generator are power, frequency, and amplitude. In terms of ultrasonic treatment of molten metals, the power range varies from 200 to 1600 watts depending on the emitting face area. For larger areas, higher power is required and vice versa. Frequency of ultrasonic treatment occurs most effectively within the range of 18 to 22 kHz. Low frequencies do not supply enough intensity for treatment to occur. High frequencies do not allow enough time for the treatment to have a lasting effect.⁶ On an ultrasonic generator, frequency is directly supported by the power and therefore the amplitude is what experiences decay. In general, there is

no relationship between amplitude and frequency and an ultrasonic wave can have any amplitude. However, in a working relationship of both frequency and amplitude being produced by the same power source, the amplitude can only be so high before adversely affecting the frequency and vice versa. Many ultrasonic generators have a fixed frequency, and the amplitude is tuned on a scale of 0 to 100% where the amplitude can be set as a percentage of the maximum. The maximum value is determined by the system's setup such as the material, shape, and size of the emission equipment.

TRANSDUCER

Electricity is supplied from the ultrasonic generator to the transducer in the form of voltage and current pulses. In the transducer these electric pulses are converted to mechanical energy, also known as ultrasonic oscillations. There are two commonly used transducer types, magnetostrictive and piezoelectric.

The magnetostrictive transducer (MST) was first used in ultrasonic treatment of metals through feeders and molds.⁶ Magnetostriction is the process that converts magnetic field energy to mechanical energy. The basic assembly of an MST is a magnet layered over a meander coil layered over a magnetostrictive patch of a select material, most commonly FeCoW alloy.⁷ This assembly connects to a transformer, waveguide, booster, and radiating surface that is in direct contact with the melt. MSTs connect to an ultrasonic generator that supplies a DC current for magnetization and an AC current for excitation. MSTs function with a supplied current that induces both permanent and variable magnetic fluxes in FeCoW. The high magnetostrictive coefficient of FeCoW causes the patch to change dimensions in resonance with the frequency of the AC current of excitation. This flux in size of the material induces longitudinal oscillations within the material that are transmitted to the transformer, then to the waveguide, and via the radiating surface into the melt. A drawback with magnetostrictive transducers is that they require a water-cooling system on the meander coil which proves challenging in molten metal applications.

Piezoelectric transducers function on piezoelectric materials. A piezoelectric material retains the property to convert electrical energy into mechanical energy and vice versa. The piezoelectric transducer is supplied with voltage pulses from the ultrasonic generator, those pulses create an electric potential under which the piezoelectric material—commonly lead zirconate titanate (PZT)—mechanically deforms and produces an oscillation.⁸ Piezoelectric transducers operate in two regimes, parallel resonance which is voltage driven, and series resonance which is current driven. Piezoelectric transducers are more common and are used in ultrasonic treatment of metals due to their simple design and ability to run without water-cooling and rely on air-cooling.

WAVEGUIDE

The purpose of a waveguide is to direct the ultrasonic wave from the transducer to the booster or directly to the probe. The waveguide operates to maintain the intensity of the wave and transmit it with minimal losses. A waveguide may be involved in the equipment design for the purpose of functionality due to the spatial and thermal separation of the transducer and the probe.

BOOSTER

The booster is designed to increase or decrease the amplitude of a wave. The booster may be designed to transmit the wave functionally from the transducer to the probe, but the primary purpose is to adjust the intensity of the wave. A booster may be required to match the impedance of the transducer to the probe. Impedance is a material specific property that affects the oscillation through contact. Eqn. (4) shows how impedance can be calculated from ρ , material density, c , speed of sound, and s , contact surface (m^2).⁶ Similar to how an electrical transformer adjusts for the best ratio of voltage to current, the waveguide adjusts for the best ratio of motion to pressure for the traveling wave by matching the impedances of these equipment components.⁹

$$z = \rho \cdot c \cdot s \quad \text{Eqn. 4}$$

PROBE

Now that the wave has been produced by the transducer and optimized by the waveguide and booster, the oscillation is transferred to the probe, sometimes referred to as the ultrasonic horn, or sonotrode. The function of the probe is to transmit the wave directly into the medium, or liquid metal. Probe design depends on three key parameters: geometry, material, and vibration modes.

In terms of geometry, oscillations are emitted longitudinally from the faces of the probe. Traditionally, probes are solid, and the oscillation is emitted perpendicular to the contact face, as illustrated in Fig. 3. In this case, the solid probe is only immersed in the liquid metal to a depth of less than 5% of the total length, typically 10-15 mm to maintain a resonant frequency (and avoid overloading).^{10,11} In contrast, in a hollow probe, oscillations can be emitted perpendicular to the longitudinal axis of the probe, as depicted in Figs. 3-5. Hollow probes come in two variations: one with one end closed and the other with both ends open. For a hollow probe with one end closed, the generated acoustic power is high, and the acoustic field is predominantly radial.¹² Such a probe can be submerged in the liquid mass to a depth of up to 30 % of the total length. On the other hand, for probes with both ends open, the acoustic field propagates radially and axially, resulting in lower acoustic power. In this case, it is recommended to insert the probe to a maximum depth of 5 to 10 % of the total length.

Probes are made from either metallic or ceramic materials. Metallic probes are commonly made of titanium, aluminum, and sometimes refractory metals such as niobium.

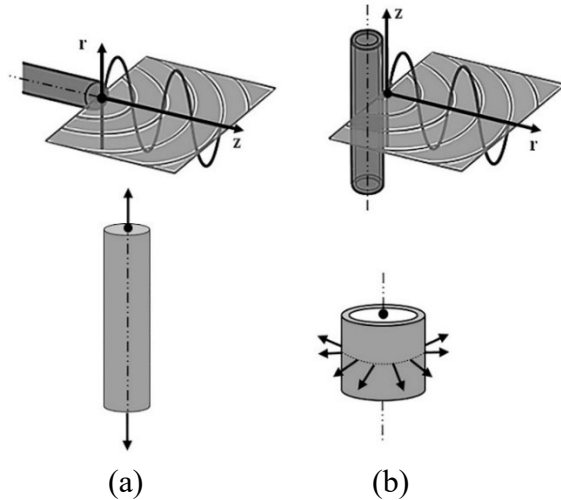


Figure 3. Solid probe sound wave emission (a) and hollow probe sound wave emission (b).

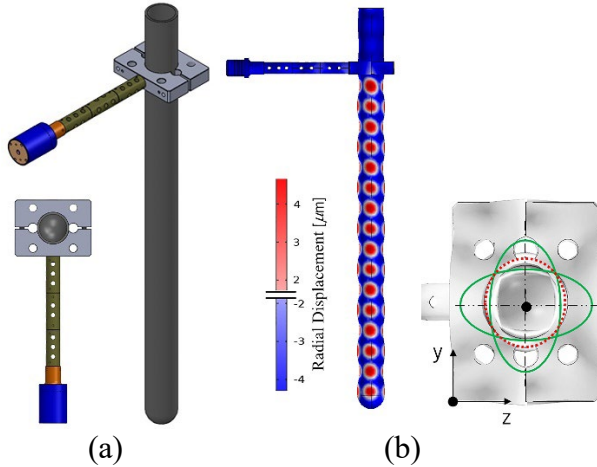


Figure 4. A hollow probe, one end open (a) and the direction of displacement radially (b).

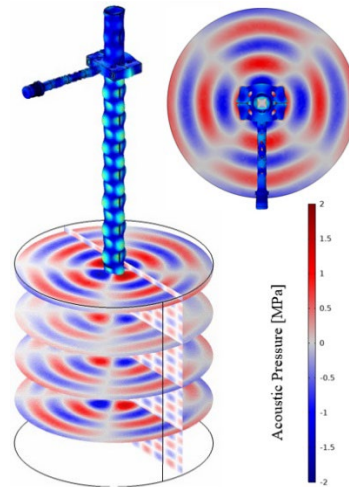


Figure 5. Concept of SiAlON Sonotrode designed to resonate at radial eigenmode (Concept created by H. Puga and Miodrag Prokic).

Niobium probes are chosen for their high temperature resistance. However, Niobium probes cannot withstand amplitudes greater than 10 micrometers and undergo erosion over time. Moreover, niobium is not cost-efficient. Aluminum is sometimes used as a probe because it is an inexpensive option, however, it must be coated with nickel or chrome to increase wear-resistance and working temperature. This option is not viable as the probe and coating erode with time. Titanium, Ti-6Al-4V, is the most common choice for metallic probes due to its relatively high melting point and mechanical toughness to withstand fracture from high frequencies. The major drawback to metallic probes is that the prolonged use of applying an ultrasonic frequency result in material erosion and potential contamination of the melt.¹³ Ceramic materials are a good choice for ultrasonic probes to be used for molten metal processing.¹⁴ SiAlON is a ceramic developed in the 1970s consisting of silicon, aluminum, oxygen, and nitrogen. For ultrasonic probe applications, β -SiAlON is used for its excellent fracture toughness, it has the chemical formula $\text{Si}_6\text{-zAl}_z\text{O}_z\text{N}_{8\text{-z}}$ where z ranges from 0 to 0.42.¹⁵ It's fracture toughness is $7.7 \text{ MPa} \cdot \text{m}^{1/2}$ which is higher than alumina at $4.5 \text{ MPa} \cdot \text{m}^{1/2}$.¹⁶ Although this fracture toughness is not as high as titanium or other metallic options which range around $30 \text{ MPa} \cdot \text{m}^{1/2}$, the wear-resistance of SiAlON is higher and thus it is less likely to erode in the molten metal.¹³

The motion (vibration mode) of a probe greatly impacts the efficiency of ultrasonic treatment. Ultrasonic waves can only travel so far into the melt and treat a specific volume due to the acoustic attenuation of the system. Probe movement enables the treatment of larger volumes because the ultrasonic source is brought closer to farther reaches of the melt. Some examples of probe motion have been tested using hollow SiAlON probes where emission

occurs at 90° angles.¹² When the probe is placed in the center of the liquid metal, it can be spiraled so that the treatment reaches the areas in between the 90° intervals. If the probe is placed off center, then the probe can be rotated around the circumference of the liquid metal and can affect the outer edges of the crucible. Alternatively, a combination of both motions—spiral and rotation of the probe may be used. The main issue with using ceramic probes is that they dominantly support radial vibration motion. This type of motion (vibration mode) has a lower amplitude compared to the axial mode, and why rotational motion is the preferred method for SiAlON ceramic tubes. As was shown in Fig. 4, the radial vibration motion induced by the imposed mechanical coupling is elliptical in nature. As a result, the probe tends to exhibit 4 planes (90° apart), where the amplitude is at its maximum value. Fig. 6 displays a perspective of these motions for hollow sonotrodes.

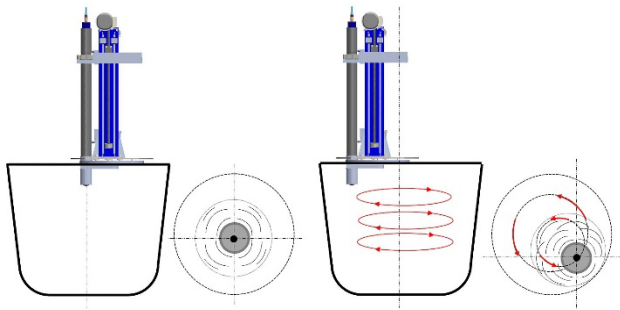


Figure 6. Two distinct types of motion: spiral and rotational, utilizing hollow sonotrodes (Concept created by H. Puga and Miodrag Prokic).

EQUIPMENT & AMPLITUDE

The three main considerations for maximizing amplitude are power supply, probe diameter, and system resonance. The power supplied is directly proportional to the amplitude and intensity of the treatment, as given by Eqn. (1).⁶ Probe diameter affects power consumption; the larger the probe diameter is, the more power is required to maintain the amplitude. However, probe diameter is also a function of the volume of melt to be treated, and the maximum potential amplitude; so, there is a tradeoff between amount of power supplied versus probe diameter. System resonance is determined by a frequency match with the distance to the nearest solid surface. If the frequency of the probe and the nearest solid surface is matched, then the amplitude of the oncoming wave and the reflected wave is constructive and forms a larger amplitude. This resonance is how a system can be configured to address the challenge of attenuation by increasing the amplitude and intensity. When the system is out of resonance, the waves are destructive and can reduce the amplitude to zero resulting in no effective treatment.

EQUIPMENT SYSTEMS

Southwire is a manufacturer of wires and cables and of metal processing equipment. Their division, SCR Technologies, has developed ultrasonic degassing equipment for use in launder systems.¹⁷ This equipment for ultrasonic treatment consists of a generator, a transducer, and a probe. The generator is a fixed 20 kHz frequency and variable 1500 W AC power supply from Sonics & Materials, Fig. 7. This generator works to maintain a constant amplitude of treatment by varying the power supplied. As the viscosity of the molten metal changes during processing, the generator increases the power supplied to ensure the amplitude of the probe is maximized, and that it remains constant. The transducer, or “converter,” is also supplied by the same firm and is rated to match the generator. The transducer contains piezoelectric material which transform the AC power into mechanical vibration. Altogether, the transducer, booster, and probe comprise what is known as the sonotrode. The transducer is the topmost part of the sonotrode, followed by the probe. The probe is made of SiAlON ceramic and is 22 mm in diameter. There are three small through-holes that run up the length of the probe so that a purge gas can flow through it for the purpose of a combination of UST and purge degassing. Although the probe was mainly aimed for degassing the melt, it is also capable of being used for ultrasonic treatment without purge gas flow for other applications such as grain refinement and intermetallic modification. Fig. 8 is a schematic diagram of the sonotrode. Larger, industry-scale equipment which uses two generators from Ducane and two adjacent sonotrodes to increase the treatable volume is also available.¹⁷



Figure 7. This generator is a fixed 20 kHz frequency and variable 1500 W AC power supply. (Photo courtesy of Sonics & Materials.)

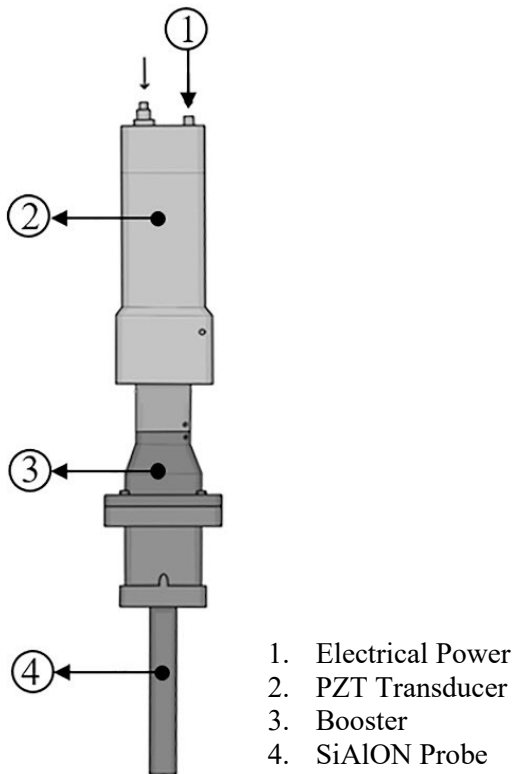


Figure 8. Schematic diagram of the sonotrode.

MP Interconsulting, (MPI), is a Switzerland based company that produces ultrasonic equipment for various applications outside of liquid metallurgy. Recently, the company has developed ultrasonic equipment for foundry applications. Considering ultrasonic physics and science of wave propagation, they developed novel utilization of amplitude and frequency to increase the effectiveness and efficiency of UST for molten metal processing. Their approach operates in a variable frequency modality, which has many advantages over fixed frequency modality. Specifically, the Multi-Frequency Mode Modulated, technology, or MMM alters the frequency as the probe is operating around the volume of the treated melt.^{16,18} MMM in liquid processing increases effects of cavitation, sonochemistry, and homogenization because standing waves are not created and the total liquid volume is uniformly agitated.¹⁶ This technology is used to optimize the system resonance and to increase the amplitude, as well as altering the frequency when the melt viscosity increases, which occurs as temperature decreases. The basis of MMM modality in UST is to maintain the highest amplitude possible via system resonance. As mentioned previously, amplitude is related to the intensity of the wave which dictates the effectiveness of the ultrasonic wave.⁶ The MPI system operates with a hollow probe which emits ultrasonic waves at 90° angles laterally. As the probe rotates around the volume of the melt the frequency supplied changes to match the wavelength of treatment to the distance between the probe and nearest solid surface. MMM is

operated via software that controls the physical motion of the probe and ultrasonic wave generation. The hollow probe is approximately 1200mm tall and 80mm in diameter. The probe can either be one-end-open or both-ends-open depending on the desired treatment (acoustic power vs acoustic field). The probe is connected to a waveguide that runs to the transducer as seen in Fig. 9.



Figure 9. The ultrasonic equipment setup. (Photo courtesy of MPI.)

MECHANISMS OF ULTRASONIC TREATMENT IN MOLTEN METALS

The mechanisms by which ultrasonic waves interact with molten metal and bring about modifications to the metallurgical quality of the metal can be categorized as either via cavitation and/or streaming. These are further detailed out below.

ACOUSTIC CAVITATION

In liquid media, the peaks of an oscillating ultrasonic wave result in two actions, compression, and rarefaction. During compression, the wave causes bubbles and gas to compress and pressurize. As oscillation continues, rarefaction sets in and causes tensile stresses within the medium. Any existing bubbles expand, and the tensile stresses form new cavities that experience compression and rarefaction in the oscillations to come. With each passing oscillation the bubbles compress more and expand more than the previous oscillation. Eventually the bubble reaches an unstable size and shape so that on the successive compression stage the bubble collapses, Fig. 10. Upon collapse, the surrounding material experiences hydraulic shockwaves with local pressures of thousands of MPa and local temperatures of up to 9000F (5000C).⁶ If the temperature is below the liquidus, the shockwave of acoustic cavitation can lead to dendrite fragmentation which will cause in-situ grain refinement.¹⁹ In the liquid

state, this mechanism results in increased mass transport due to the turbulence of cavitation.

Acoustic cavitation is an intensity dependent mechanism.⁹ During a low intensity treatment, the wave functions in a “pre-cavitation” mode in that bubbles form, compress, and rarefaction is occurring, however the bubbles do not collapse. There is a cavitation threshold value that is material specific and depends on the ultrasonic wave intensity; below the cavitation threshold is when the bubbles do not collapse, the “pre-cavitation” mode. This mode can occur at both low and high frequencies; intensity is dependent on the frequency – Eqn. (1). At low frequencies, the intensity is insufficient and there is not enough power per surface area to cause the bubbles to reach that unstable shape and size for collapse. At high frequencies, the intensity is sufficient, but the oscillation period is not long enough for the bubble to collapse. In this case the bubbles are supplied with enough power to reach an unstable size, but before collapse can occur the bubble is already entering the next stage of rarefaction. Pre-cavitation in the liquid state leads to bubble formation

and aggregation, and subsequently the bubbles rise to the surface and escape the melt (degassing).

Cavitation bubbles grow in predictable locations known as cavitation nuclei. Cavitation nuclei grow at “weak points” in the liquid medium where there is a difference in surface tension or separation of material. The interface between two immiscible liquids, the complex surfaces of particles, and other gases or insoluble impurities are examples of cavitation nuclei. These interfaces and surfaces become weak points because they have a low wettability in liquid Al. Due to their low wettability, these locations have a high propensity for hydrogen collection. Aluminum oxide, Al_2O_3 , is pervasive in all molten Al processing, and the oxide mixes into the melt volume and has poor wettability with the melt. Hydrogen adsorbs on the surfaces of these oxide particles. Within a given melt of liquid aluminum, 0.005 % of Al_2O_3 particles controls about 5 % of all dissolved hydrogen in the volume via this mechanism.⁶ When ultrasonic treatment is applied, the adsorbed hydrogen is influenced by the oscillation into cavitation.

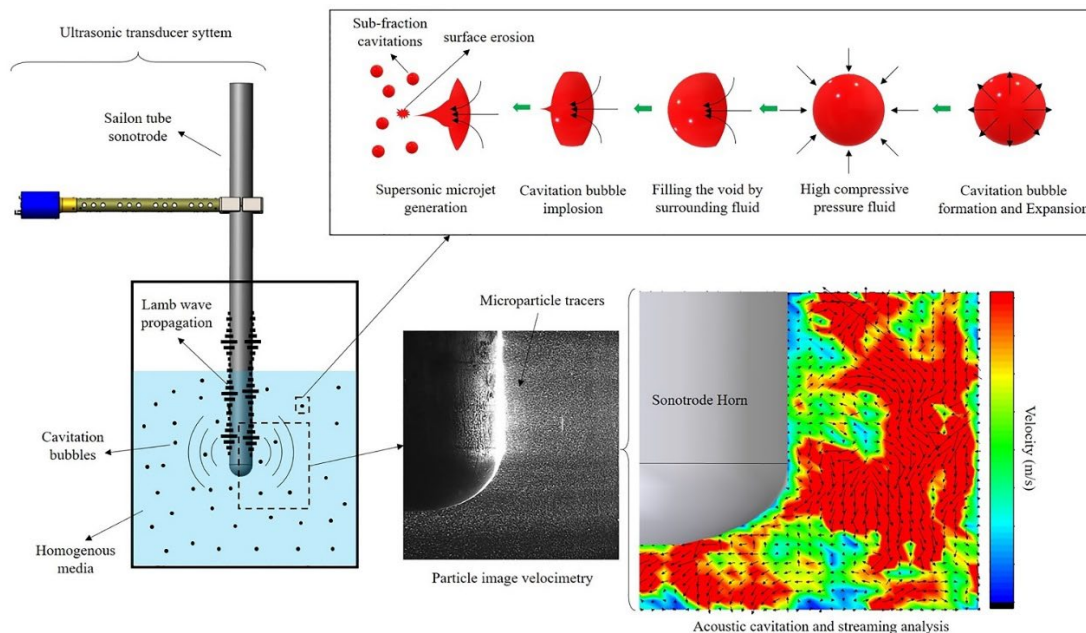


Figure 10. A visual representation illustrating how an ultrasonic wave generates compression and rarefaction, leading to acoustic cavitation.

ACOUSTIC STREAMING

Acoustic streaming occurs in two ways: (i) streams that form directly due to the ultrasonic energy absorption, and (ii) streams following the collapse of bubbles from acoustic cavitation. As ultrasonic energy is absorbed by the melt, streams form in viscous layers near solid boundaries or phase interfaces in fields of standing waves away from the boundary layers; streams form from the absorption of wave momentum. After the collapse of a bubble caused by acoustic cavitation, the streams that form cause liquid material to rush into the regions where the bubble imploded with velocities of hundreds of m/s.

Streams that result directly from the energy of an ultrasonic wave are slower than those of acoustic cavitation, but these streams are sped up once cavitation sets in. Acoustic streams form closed loops whose size is inversely proportional to the acting wave's frequency.⁶ The combination of the high temperature and high pressure of acoustic cavitation with the high velocity travel of acoustic streaming results in a homogenous distribution of material and temperature. During continual operation the streams continue, loops combine and form larger homogenous loops that orientate themselves lengthwise in an oval shape from the ultrasonic source,

Fig. 8. In the liquid state, both stream types result in increased mass transport along these stream loops. In the liquid-solid state, the streams impact solidifying surfaces and result in surface damage or dendritic fragmentation, after which these fragments can be transported as new nuclei for heterogeneous nucleation.

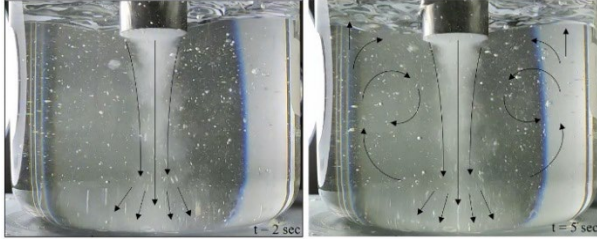


Figure 11. The formation pattern of acoustic streaming loops in relation to the location of the ultrasonic source at $t=2$ seconds (left) and $t=5$ seconds (right).

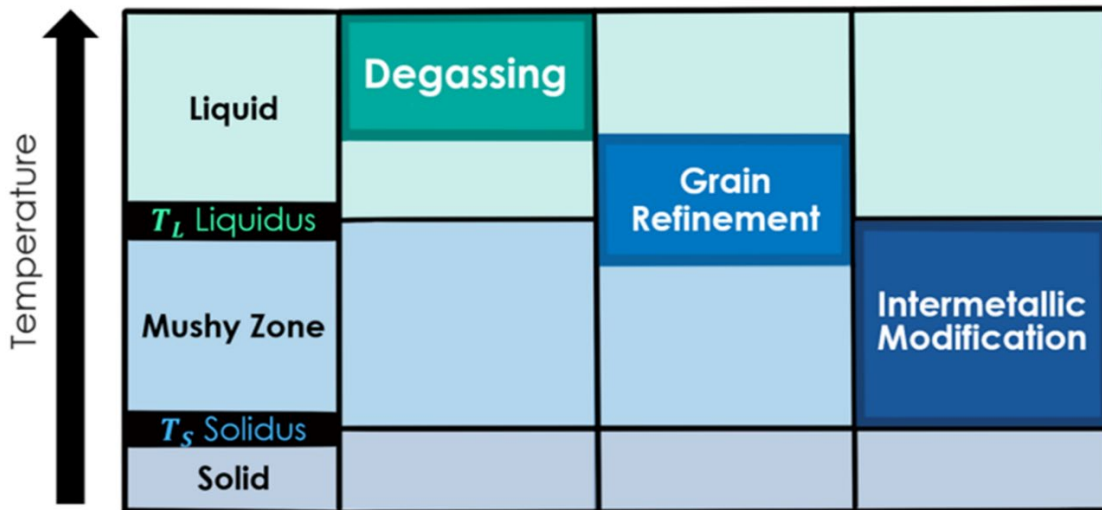


Figure 12. Preferential treatment temperature ranges for UST degassing, grain refinement, and intermetallic modification.

When treatment is applied above the liquidus temperature, the dominant effect of the ultrasonic energy is the creation of cavitation bubbles and large streaming loops which encompass the entirety of the treatable volume. The combination of these two effects results in UST being an efficient degassing technique. As the temperature lowers and approaches the liquidus temperature, UST streaming loops are flowing to homogenize the composition all the way to the onset of solidification. This effect alters the formation and the morphology of the first solidifying phases, which can be beneficial in modifying the morphology of iron-based intermetallic phases. The cavitation bubbles and streaming loops that are formed via ultrasonic energy impact the solidified interfaces and cause fragmentation. The fragmented particles are redistributed by the streaming loops and act as nucleation sites in new locations and thus in-situ grain refinement. Grain refinement may also be attained in the fully liquid

ULTRASONIC TREATMENT APPLICATIONS

At the onset, it is important to distinguish between ultrasonic treatments (UST) by the temperature of the metal or the medium. Ultrasonic treatment is either carried out in the fully molten state (above the liquidus), or slightly below the liquidus temperature (5-10% fraction solid), and if appropriate probes are utilized, at temperatures in the mushy zone (10-20% fraction solid). Degassing and mixing for metal matrix nanocomposites is possible in the fully liquid state while grain refinement and intermetallic modification occur with some amount of fraction solid. Fig. 12 displays the temperature ranges that work successfully for their respective UST applications.

state via broken oxides rather than fragmented solidified phases.

DEGASSING

The solubility of hydrogen in molten Al is ~1 mL/100 g versus 0.05 mL/100 g in the solid state. If the hydrogen is not removed from the molten metal before solidification, gas porosity significantly impairs the resultant mechanical properties.^{20,21} Trapped hydrogen within the solidified metal exists in the form of porosity. Pores in the solidified casts act as weak points for fracture and failure, as do inclusions and oxides. Fig. 13 shows the effect of degassing on porosity and the correlation of porosity to ultimate tensile strength in Al-4.5%Cu, Al-11%Mg, and Al-5%Si. As the porosity percentage increases, the ultimate tensile strength decreases.

Accordingly, a key molten metal processing technology for Al is degassing. The procedure involves an inert purge gas, such as argon or nitrogen, that bubbles into the lower

portion of the melt through a rotating impeller. The rotating impeller intakes liquid aluminum from below and forces mixing with the purge gas. Dissolved hydrogen within the melt diffuses into the gas bubbles, which then float upwards and carry the diffused hydrogen to the surface. The rotating impeller also breaks up oxides which float upwards to the surface of the melt.^{22,23} Figure 14 shows the benefits of degassing on mechanical properties in an Al-Si-Mg alloy dependent on traditional rotary degassing conditions. Overall, there is an increase in the tensile strength of the alloy when compared to non-degassed samples.

When an ultrasonic wave is applied to a fully liquid melt, cavitation bubbles form as well as full-circuit streaming loops. As cavitation bubbles form, hydrogen from within the melt dissolve into the bubbles, which are then swept up by the streaming loops and brought closer to the surface until they reach a minimum depth from which the hydrogen can escape. This is the basis of how UST can degas a liquid metal. This mechanism is visualized in Fig. 15. However, UST can be applied for degassing purposes in various ways: (i) UST solely applied without any additional inputs; (ii) UST with variable frequency capability; and (iii) UST in combination with a purge gas.

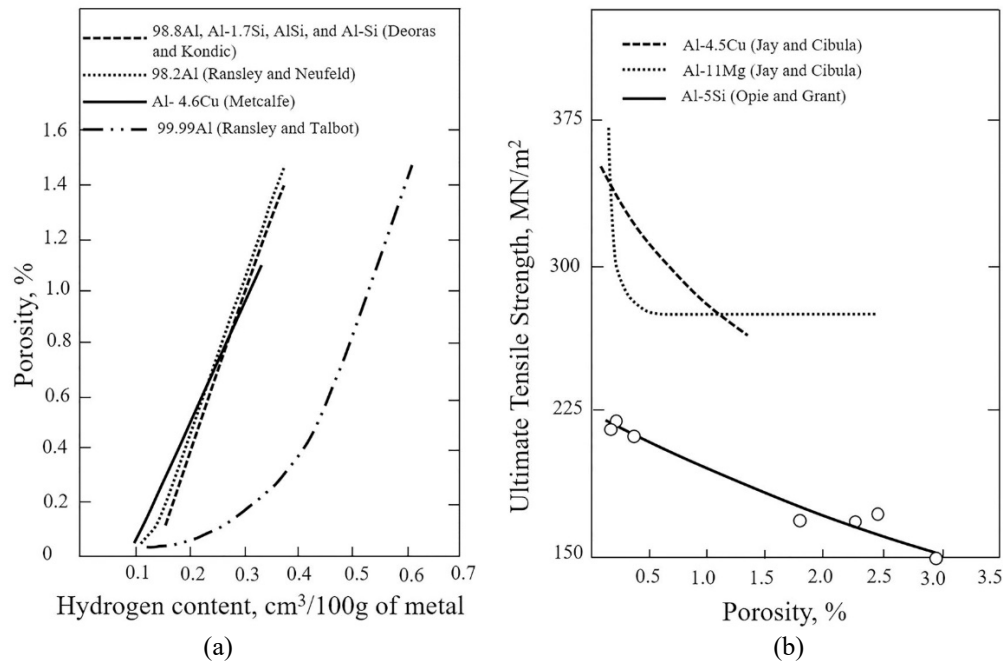


Figure 13. The correlation between hydrogen content and porosity in various aluminum alloys (a) and the correlation between porosity and ultimate tensile strength in various aluminum alloys (b).²¹

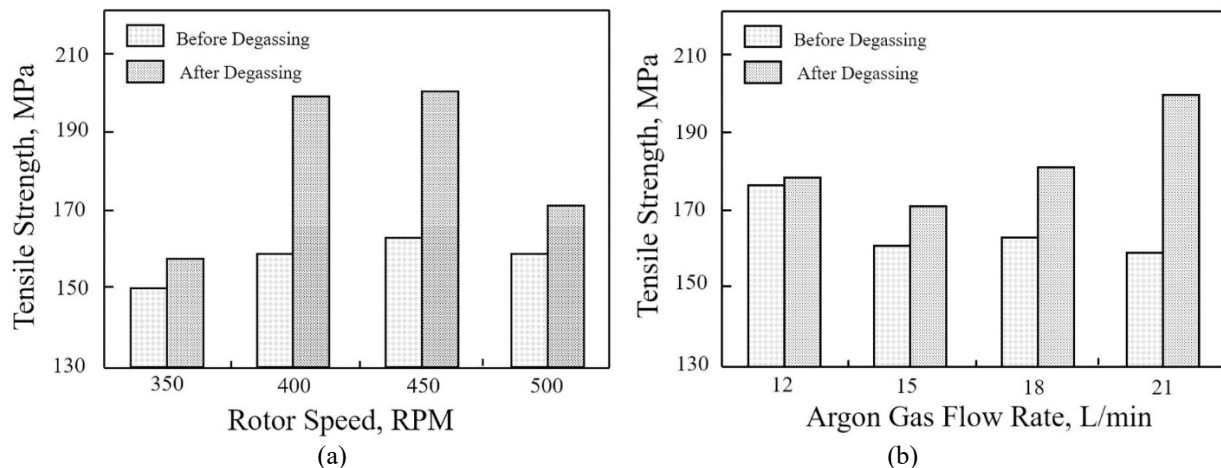


Figure 14. The effect of traditional rotary degassing parameters of rotor speed (a) and argon gas flow rate (b) on tensile strength.²⁴

Recently, H. Puga, with MPI MMM technology, developed a prototype that allows the combination of mechanical rotation of the system with dynamic ultrasonic agitation. This system increases the efficiency of the metal treatment in cases with large material volumes, low treatment temperatures, or reduced levels of dissolved hydrogen in the medium. Moreover, it has been reported that using UST in MMM modality or in a variable frequency mode obviates the need to use a purge gas during degassing.¹²

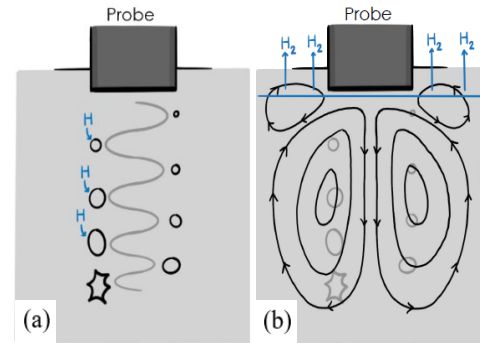


Figure 15. A visual of how UST alone causes degassing of hydrogen via (a) hydrogen dissolving into cavitation bubbles and (b) streaming loop transportation of hydrogen filled cavitation bubbles.

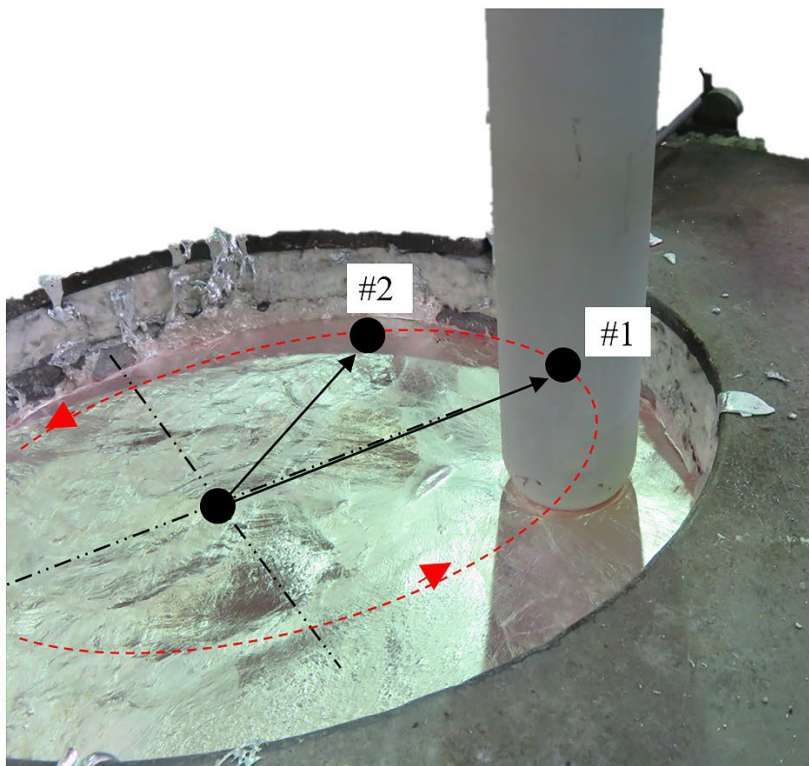
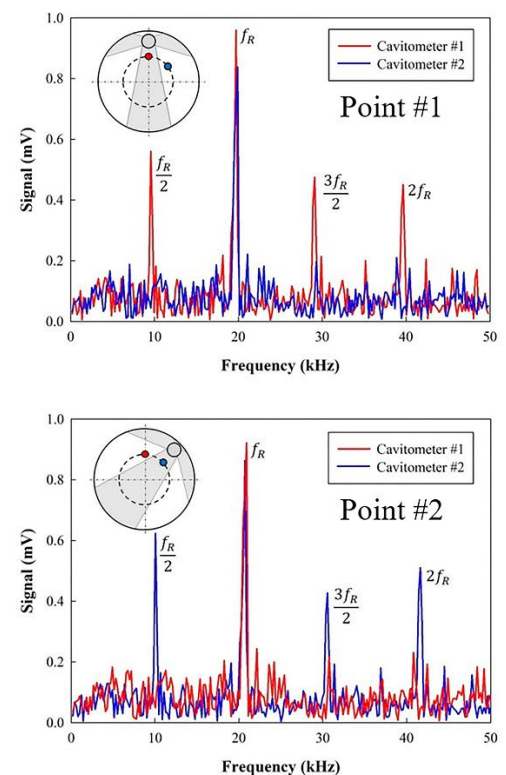


Figure 16. Experimental apparatus for the ultrasonic ceramic sonotrode translation. Level of cavitation registered at Point #1 and #2 - adapted from Reference #12.

Figures 17 and 18 show the results of three different degassing methods in terms of hydrogen content and alloy density, respectively. MMM UST degassing and MMM UST degassing with rotation both showed a lower hydrogen content post-processing when compared with traditional argon rotary degassing within the first two minutes. MMM UST procedures reaches a lower steady state hydrogen content in less time than traditional rotary degassing, in accordance with MPI data. A reduced pressure test also showed the comparison of traditional with UST degassing for increases in the alloy density with respect to degassing time.¹²



UST can also be combined with a purge gas to increase degassing efficiency. Southwire Corp. provides ultrasonic degassing equipment (Ultra-D Degasser) consisting of a ceramic SiAlON solid probe containing three small holes that run through the probe lengthwise. These through-holes allow for the use of a purge gas into the liquid metal in the same direction that the ultrasonic wave is applied into the melt. The basis of this mechanism is that in addition to cavitation bubbles acting as a sink for hydrogen, the purge gas also enhances and complement diffusion of hydrogen to the bubbles. The conceptual

framework of this approach is that a combination of cavitation bubbles and purge gas bubbles can interact with more of the melt and thus enhance the efficiency of hydrogen removal. This combination of bubbles is then removed by the streaming loops as discussed.

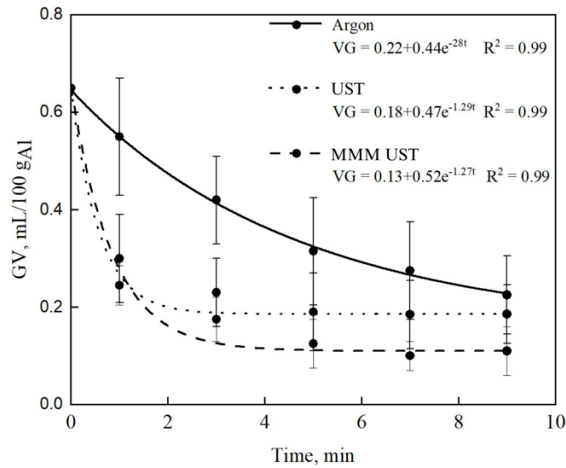


Figure 17. MMM results of hydrogen removal in AISi9Cu3(Fe) alloy using traditional argon rotary degassing, UST degassing, and MMM UST degassing and with probe rotation.¹²

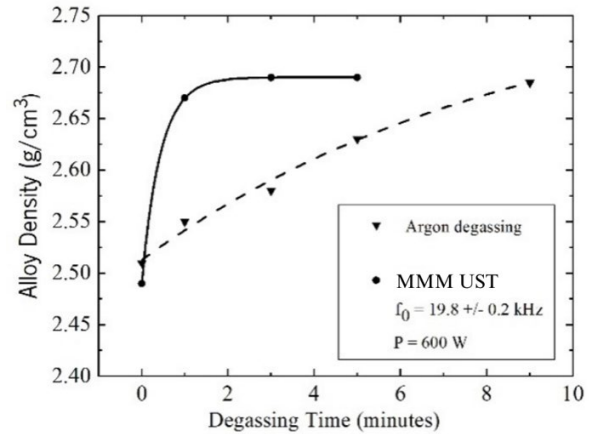


Figure 18. Alloy density vs. degassing time as plotted for MMM UST degassing (solid) and for traditional argon rotary degassing (dashed).¹²

Table 1 shows results from a study of UST and purge degassing in a twin-roll casting launder.²⁵ Three conditions were studied. The condition titled “Not optimized” refers to no degassing and thus no efforts were made to lower hydrogen or oxide content. The condition titled “1st Step” refers to methods to reduce turbulence at the surface of the liquid metal to prevent the entrapment of oxides and inclusions. This 1st Step increases hydrogen removal efficiency from 45% to 60%. The condition titled “2nd Step” is when purge gas and ultrasonic treatment are carried out together in the launder. The latter increased the removal efficiency from 45% to 77.8%. Figure 19 shows the effect of UST and purge degassing on inclusion and oxide content, which were measured using Porous Disk Filtration Analysis (PoDFA), before and after degassing. Both the oxide films and the various inclusion concentrations were decreased significantly, including the chemical grain refiner.²⁵

Table 1. Southwire Results on Degassing that Compare Unoptimized System As-Cast, to 1st Step Optimized System, to 2nd Step Optimized System Involving UST in Combination with a Purge Gas²⁵

Condition	Location	Hydrogen ml/100g	Temperature °C	Removal Efficiency
Not optimized	Furnace Exit	0.40	760	45.0 %
	After Filter	0.22	706	
1st step	Furnace Exist	0.40	760	60.0 %
	After Filter	0.16	707	
2nd step	Furnace Exit	0.45	791	77.8 %
	After Filter	0.16	708	

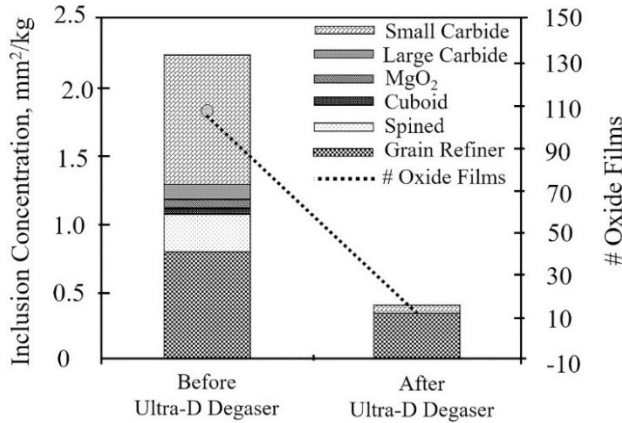


Figure 19. Inclusion concentration before and after degassing with the Southwire degassing system.²⁵

Fixed frequency ultrasonic treatment has been studied with respect to multiple system conditions. A study by T. Meek et al. investigated the effects of humidity, treatment temperature, and melt volume on the effectiveness and efficiency of UST degassing²⁶. The experimental setup included a fixed frequency 20kHz ultrasonic generator, a PZT transducer, and a Ti-6Al-4V probe. Their study on humidity evaluated treatment of 0.2 kg of A356 at 1364F (740C) for two different humid environments, 40 % and 60 %. The results recorded hydrogen content in the melt with respect to UST degassing time, as seen in Fig. 20. Their conclusion was that the change in humidity of the environment does not affect the lowest achievable hydrogen content.

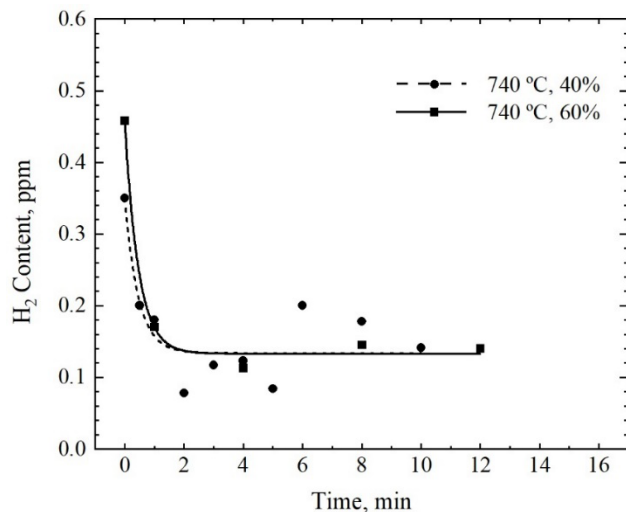


Figure 20. Hydrogen content per UST degassing time in 40 % humidity (dashed) and 60 % humidity (solid).²⁶

Regarding the effect of temperature, Meek et al. investigated treatment at four different temperatures for relatively the same humidity. A356 has an approximate liquidus temperature of 1139F (615C). These trials studies

treatment at 1148F (620C), 1202 F (660C), 1292F (700 C), and 1364F (740C). The recorded hydrogen content per UST degassing time showed that UST degassing at temperatures closer to the liquidus temperature took significantly longer to reach the lowest steady state hydrogen content, Fig. 21. Treatment at different temperatures did not reach the same lowest steady state hydrogen content. At 1148F (620C) the lowest was not reached during the 20-minute trial. At 1202F (660C), the lowest steady state hydrogen content took approximately 3 minutes to reach and was lower than what was achieved at 1292F (700C) which reached the lowest steady state hydrogen content within approximately 1.5 minutes. At 1364F (740C) the steady state hydrogen content was the lowest of all the trials and was reached in approximately 1.5 minutes.²⁶ These data contradict what is observed in traditional rotary degassing. Traditional rotary degassing is most efficient at lower temperatures because the influx of hydrogen at the surface is minimized with lower temperatures. The data in Fig. 21 shows the opposite, that for UST degassing a higher temperature is favored. This can be explained via the viscosity of the metal being treated. As the temperature drops, the viscosity of molten metal increases. When the viscosity is raised, ultrasonic energy is dampened and absorbed sooner than in a lower viscosity melt, thus reducing the effective treatment.

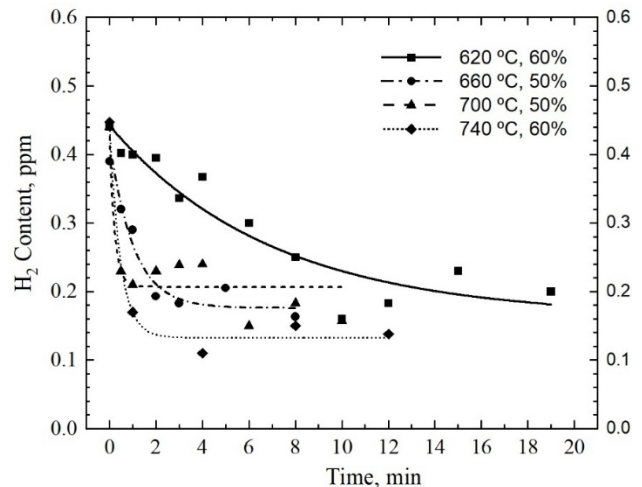


Figure 21. Hydrogen content per UST degassing time at 1148F (620C), 1202F (660C), 1292F (700C), and 1364F (740C).²⁶

The study on different volumes of melt investigated UST degassing of a 0.2 kg, 0.6 kg, and 2.0 kg melt. All trials were treated at 1292F (700C) and 60 % humidity. As the size of the melt increased, the time required for UST degassing increased, as expected. Fig. 22 depicts how the melts reach a relatively similar steady state hydrogen content. A 0.2 kg melt reached steady state within 2 minutes while a 2.0 kg melt reaches steady state after 6 minutes. The conclusion made was that regardless of melt size, a similar steady state hydrogen content is possible with different UST degassing times.²⁶

Table 2. Amount of Dross Production (Grams) for Traditional Degassing and UST Purge Degassing with Respect to Degassing Time²⁶

Degassing Method	Degassing Time (min)					
	2	5	10	15	20	25
Argon Degassing Alone	NA	16.6	22.8 ^a	39.4	49.5	65.1
Argon Degassing with Ultrasonics	0.9	1.8 ^a	5.2	6.4	NA	NA

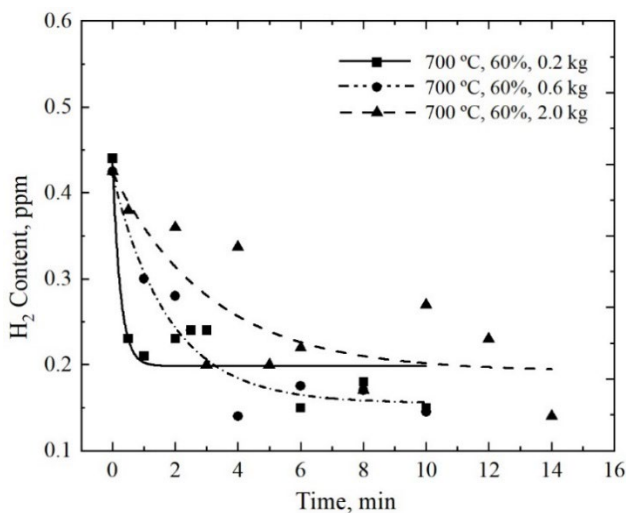


Figure 22. Hydrogen content per UST degassing time in 0.2 kg, 0.6 kg, and 2.0 kg.²⁶

Meek's study claims that UST degassing with a purge gas significantly decreases the amount of dross formation²⁶. UST purge degassing functions through the introduction of a purge gas during UST. The presence of a purge gas is suspected to increase the survival and presence of bubbles that ultrasonic energy can act on in the melt. Table 2 shows the amount in grams of dross produced via traditional argon degassing and UST purge degassing for a specified degassing time for a 5.0 kg melt of A356. At every time there is significantly less dross produced with UST purge degassing than there is for traditional rotary degassing.

A recommendation for future research is to study the formation of a cavitation bubble and determine the composition inside the bubble, which is a difficult task. It is commonly believed that cavitation bubbles form around weak points in the melt such as hydrogen that is adsorbed to the surface of an oxide or inclusion or that the bubbles fill with aluminum vapor during the stages of cavitation.⁶ For the first reason to be the case, there would have to be a minimum hydrogen content for cavitation bubbles to

form in molten aluminum. This is a path of study that should be pursued to mechanistically define cavitation and develop an optimum process for UST degassing. UST purge degassing should be compared with UST degassing alone in terms of dross production and lowest possible steady state hydrogen content.

INTERMETALLIC MORPHOLOGY MODIFICATION

The presence of deleterious intermetallic compounds reduces the mechanical properties of the cast product. Intermetallic phase morphology, i.e., size and shape, is influenced by the composition as well as processing conditions. The 3XX series Al alloys are a good example, wherein harmful intermetallic compounds form due to the presence of both silicon and iron. The β -phase, or Al_5FeSi , forms early-on during solidification and with a large enough iron content, this phase experiences unrestricted growth. The β -phase forms in a platelet morphology, which on a 2D micrograph can be observed as needles.²⁷ The Al_5FeSi needles are hard, brittle, and serve as crack-initiation sites.²⁸ The α -phase, or the $\text{Al}_8\text{Fe}_2\text{Si}$ phase, forms before the β -phase and has a unique 'crinkled' shaped. This phase causes less harm on mechanical properties than the β -phase, however it is still an undesirable phase. Figure 23 shows the size and shape of the β -phase as well as the α -phase in an Al-Si-Fe alloy.

In terms of modifying the morphology of these intermetallic compounds, there are few procedures to regulate their growth. A common technique for alloy systems where the iron content is 0.45 wt% iron or more is to maintain a minimum 2:1 ratio of iron to manganese in the alloy.^{24,29} The manganese presence in this ratio restricts the formation of the β -phase by producing more of the α -phase first and exhausting more iron in this formation.³⁰ This method lowers the amount of β -phase and improves mechanical properties minimally as the presence of the α -phase is still detrimental to mechanical properties. The consequence of this technique is that the addition of manganese increases the amount of slag production. Cooling rate provides another method of

regulating the size and morphology of these iron based intermetallics. A fast-cooling rate restricts the total size that the intermetallic can grow to since the intermetallics are the first phases to solidify.³¹ Intermetallic growth can be controlled effectively by synchronizing cooling rate and manganese content as seen in Fig. 24. In general, a

higher cooling rate and moderate manganese content produces a less harmful β -phase morphology. Although this is an effective method of regulating intermetallic growth, it is unfortunately a new restriction both compositionally and process-wise.

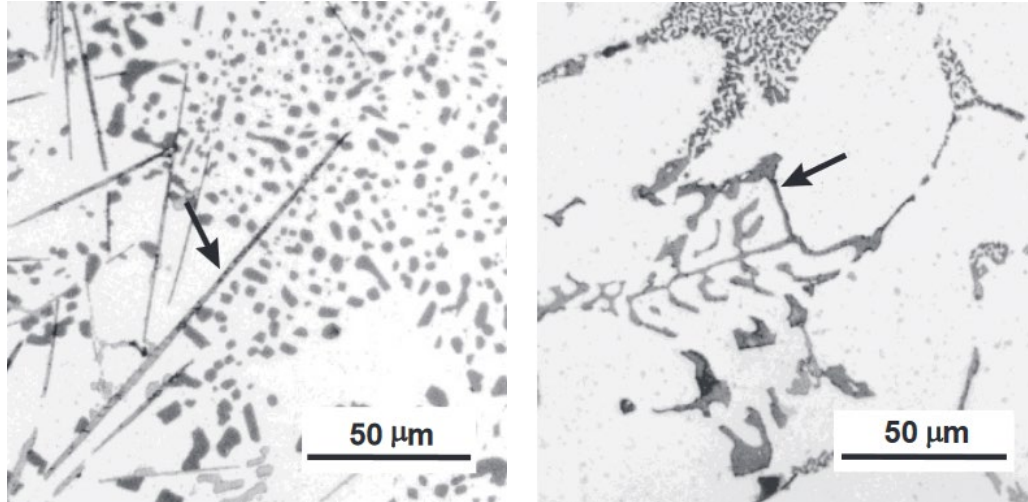


Figure 23. Micrographs of an Al-5Si-1Cu-0.5Mg-(Fe) alloy showing the β -phase (left) and the α -phase (right).²⁷

Another method is 'intensive melt shearing' in which there is mechanical shearing of the molten metal using a rotor.^{32,33} The rotor is placed in molten metal and operated at a temperature prior to the onset of solidification. Here, the melt-shearing occurred immediately before injecting the metal into an HPDC die. Figure 25 shows the effect of melt-shearing on both the amount and morphology of the β and α -phases. There are less β -phase compounds present, and the β -phase is smaller and thus less harmful than in the as-cast condition. The α -phase has also changed its morphology and there appears to be more α -phase than the as-cast counterpart.

Techniques for intermetallic modification are effective, however, they exhibit restrictions on the composition and/or processing method of the cast-part. The use of UST to modify intermetallic morphology is a recent development which is being actively investigated at the Advanced Casting Research Center (ACRC) at the Univ. of California, Irvine. The concept is based on the capability of intermetallic phase morphology to be altered

by shearing forces and the ability of ultrasonic waves to exhibit shearing action in a liquid or slurry.

The method by which ultrasonic waves refine the morphology of intermetallics can vary dependent on the temperature of treatment. Intermetallic phases in molten aluminum such as the β -Al₅FeSi or α -Al₈Fe₂Si form at the forefront of solidification in the system. Traditionally, literature has shown ultrasonic treatment to be applied below the liquidus temperature, after the primary intermetallic phases have begun to solidify. In this method of intermetallic modification via UST, both acoustic streams and acoustic cavitation work together to fragment the formed intermetallic phases. Figure 26 shows the effect of UST on a hypereutectic Al-Si-Fe alloy. The intermetallics in the UST sample are simply the fragmented and broken-up versions of the intermetallics seen in the as-cast sample. This Al-17Si-4Fe alloy has an expected liquidus temperature of 1274F (690C) and treatment was applied below that during the fully mushy zone starting from 1247F (675C) and ending at 1211F (655C) before the solidus temperature of 1076F (580C).²⁸

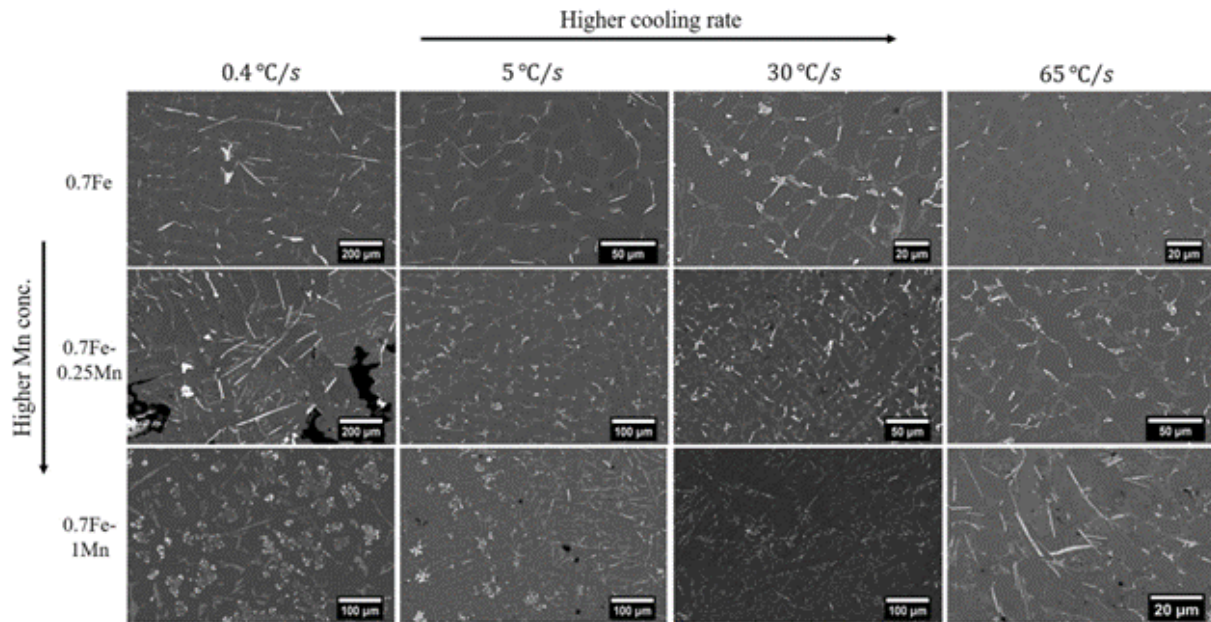


Figure 24. An array of microstructural changes in the Al-8Si-0.35Mg-0.7Fe alloy with both increases in cooling rate and increases in manganese concentration from the top left to bottom right.³¹

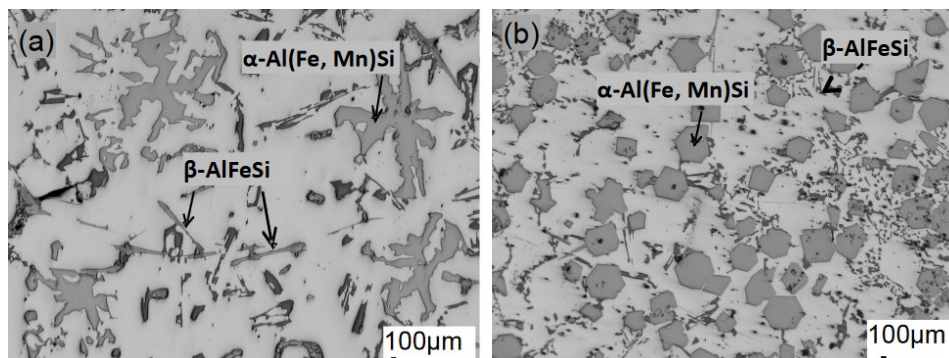


Figure 25. An LM24 (Al-Si-Cu) alloy cast at 1193F (645C) without melt-shearing (a) and with melt-shearing for 60 seconds (b).³³

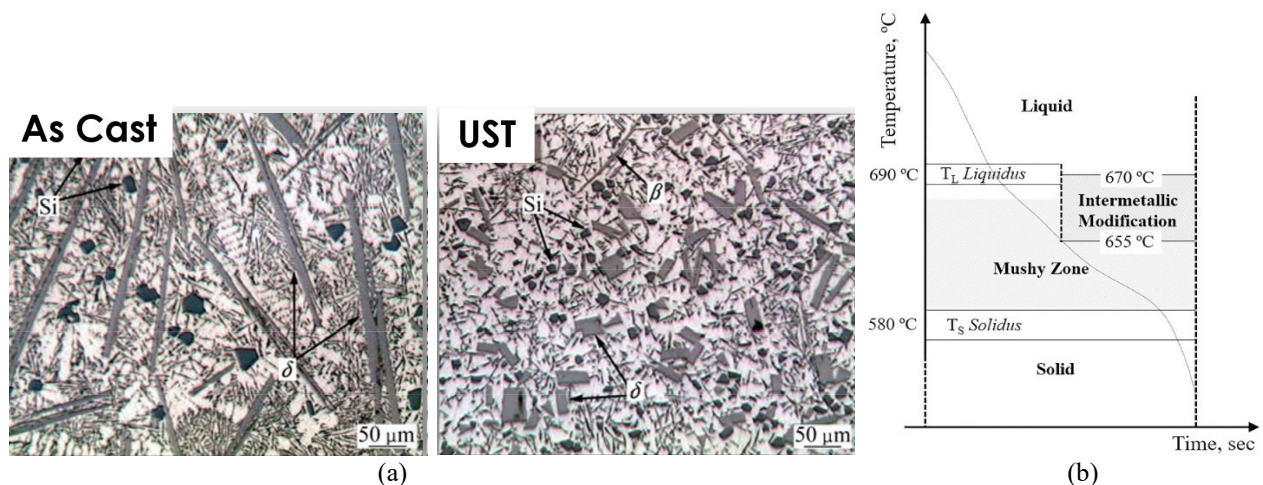


Figure 26. Al-17Si-4Fe samples with and without ultrasonic treatment²⁸ (left) a visual representation of the UST application temperature range (right).

A study on hypereutectic Al-19Si-4Fe alloy by C.J. Todaro et. al, investigated the formation of intermetallic phases with and without ultrasonic treatment¹¹. Todaro carried out UST treatment at 1274F (690C) which is above the liquidus temperature of 1229F (665C) and ended the treatment at 1130F (610C). Figure 27 displays the microstructural change from the as-cast to the UST treated sample. To explain the effect of UST on the intermetallic formation, it is useful to compare this microstructural change to that of Fig. 26 where the Al-17Si-4Fe alloy was treated below the liquidus

temperature. This implies that the intermetallic phases formed were subsequently broken up by the applied ultrasonic energy. This is visible in Fig. 26 where the as-cast samples have long, sharp, plate-like phases and the UST sample has small chunks. This can be explained by the mechanism of phase fragmentation. When the temperature dropped below the liquidus, the intermetallic phase formation commenced. As UST was applied, these long intermetallic phases were fragmented into smaller pieces.

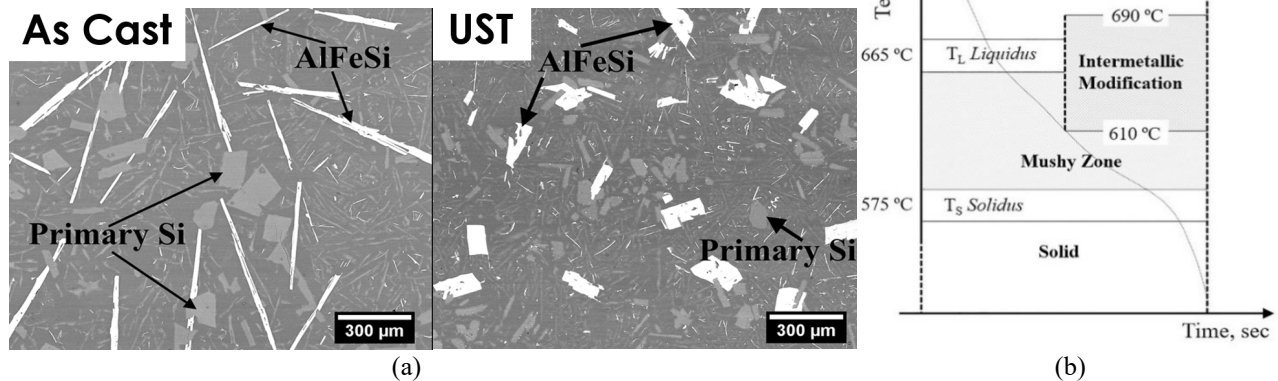


Figure 27. Al-19Si-4Fe with and without ultrasonic treatment¹¹ (a) a visual representation of the UST temperature range (b).

However, the microstructural change in Fig. 27 cannot be explained by the mechanism described above. Instead of smaller pieces that were clearly fragmented (Fig. 26), the UST sample in Fig. 27 shows that the intermetallics were not fragmented but underwent a different formation mechanism. Todaro et. al, explains this via the peritectic transformation of the δ -Al₃FeSi₂ into β -Al₅FeSi. In the as-cast alloy, the intermetallic plate-like phases are the β -Al₅FeSi that envelope the δ -Al₃FeSi₂.¹¹ This means that the peritectic transformation did not go to completion as seen in Fig. 28.

UST assisted peritectic transformation may also cause changes in the formation of different intermetallic phases in other alloy systems. For example, the A380 alloy contains up to 1.3 wt% iron and has an approximate liquidus temperature of 1100F (593C) and a solidus temperature of 1000F (538C). Figure 21 shows the Scheil solidification profile for Al alloy with Si 8 wt%, Fe 1.3 wt%, Mn 0.5 wt%, Cu 0.2 wt%, Mg 0.4 wt%, Zn 0.1 wt%, and Ti 0.2 wt%. The “Al₉Fe₂Si” phase is the β -Al₅FeSi and is calculated to be the first phase to solidify. The high iron content is responsible for the immediate and long formation of the detrimental β -Al₅FeSi. When ultrasonic treatment is applied in the melt, acoustic

streaming occurs and as the melt approaches the liquidus temperature, compositional diffusion induces the precipitation of iron-based intermetallic compounds. However, the introduction of ultrasonic energy disrupts this diffusion via acoustic streaming. This streaming alters both the size and morphology of the intermetallic compounds forming within the melt. Acoustic streaming causes the melt composition to homogenize and therefore less of the required composition is available in one location to form these intermetallics. This decrease in available composition results in the intermetallic compounds such as the β -phase being smaller and more closely dispersed rather than larger and farther apart. Similarly, as ultrasonics continue to be applied to the melt from before to after intermetallic phase formation, the compositional diffusion that occurs during phase formation is assisted and altered which affects the resultant morphology.

Future studies for the intermetallic morphology modification via ultrasonic energy should aim to define parameters necessary to affect the formation of these intermetallic phases. A study on the required temperature treatment range would further explain the mechanisms that occur to affect intermetallic formation.

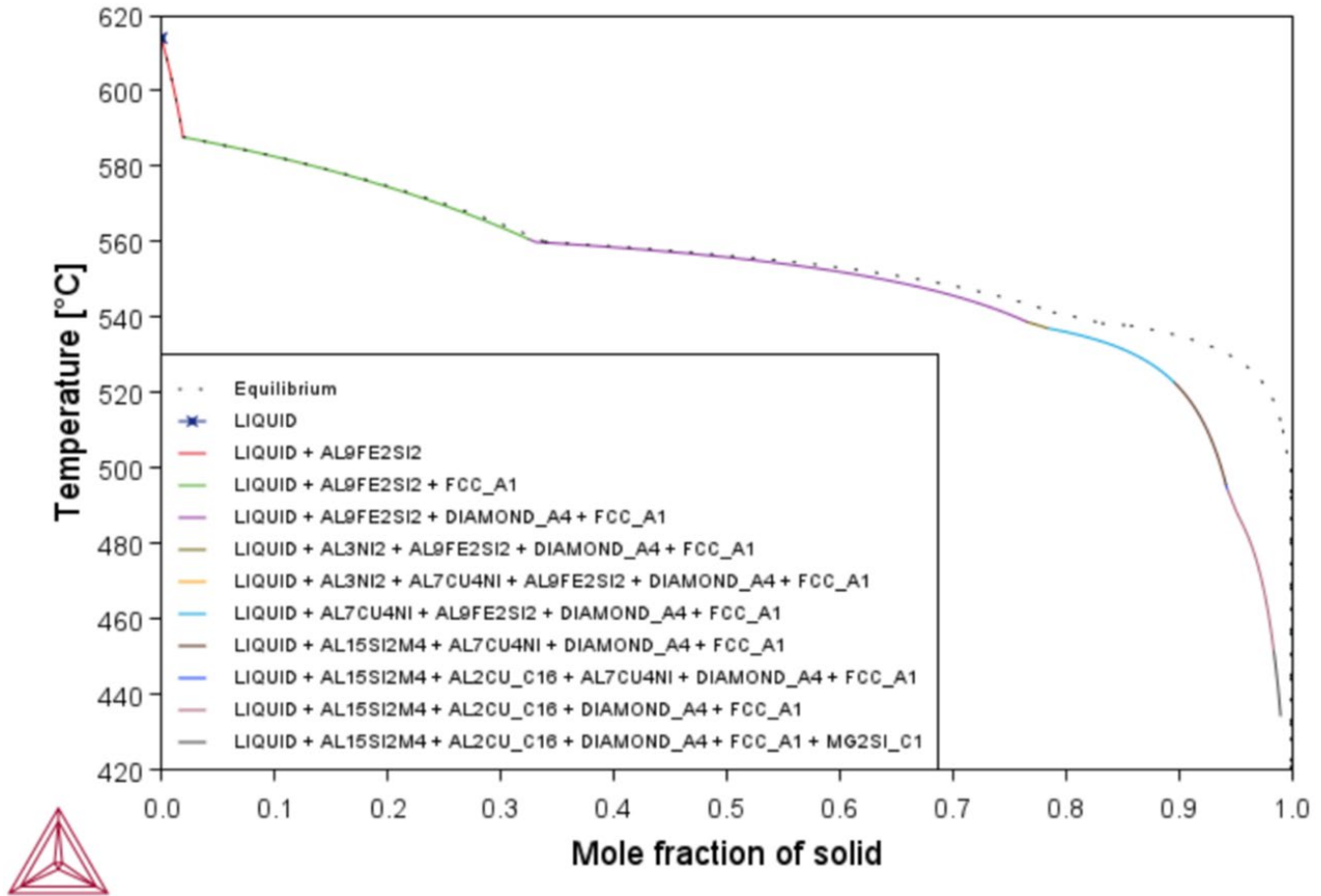


Figure 28. A Scheil solidification curve for an example A380 composition.

GRAIN REFINEMENT

Grain refinement is achieved via the addition of grain refiners such as titanium boride to the molten metal. Grain refining rod master alloys made of Al-5Ti-B are commonly added to A365 in 0.5 wt%.³⁴ Grain refiner particles act as nuclei for heterogenous nucleation.

Ultrasonic treatment can grain refine the melt without the addition of external agents. The bubble collapse that results from acoustic cavitation exerts force on solidifying interfaces which leads to fragmentation of oxides at high temperatures and dendrites at low temperatures.¹¹ The high velocity streams that follow cavitation bubble collapse also exert forces on solidifying dendrites leading to fragmentation. These dendrite fragments are further broken down by these two mechanisms and are carried by acoustic streaming around the melt volume. As

solidification continues, these fragments act as nucleation sites for heterogenous nucleation, resulting in a fine and globular structure.⁶ Ultrasonic treatment is an effective in-situ grain refiner without the addition of external agents.

Fig. 29 shows the effect of ultrasonic treatment and the resultant refined the microstructure of A356 treated at 1238F (670C)³⁵. In the same work, it was found that the constituents of the eutectic phase were modified subsequent to ultrasonic treatment. Table 3 displays the mechanical properties of brass samples produced via different refining processes. The mechanical behavior of the cast brass shows an increase through chemical refinement and similarly there is an increase through ultrasonic treatment.³⁶

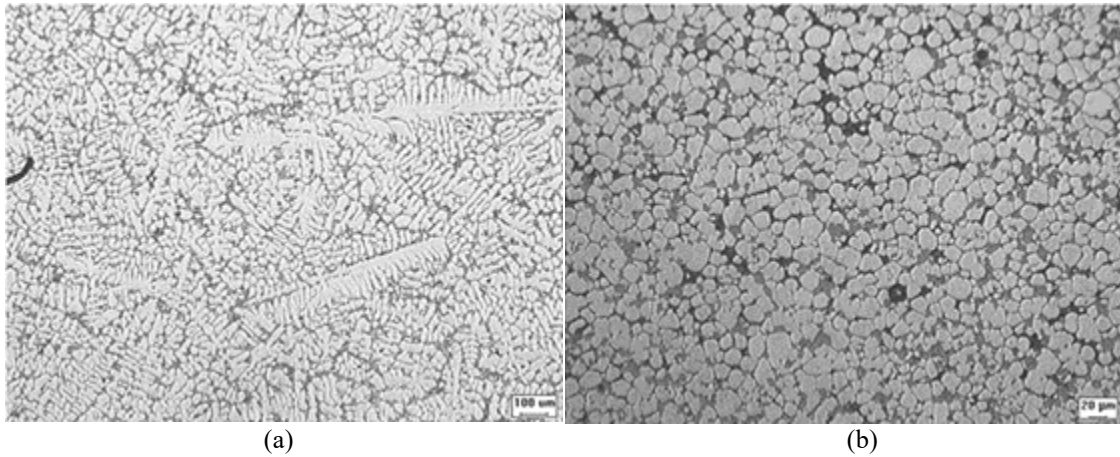


Figure 29. The microstructure of untreated A356 (a) and the microstructure of UST grain refined A356 (b).³⁵

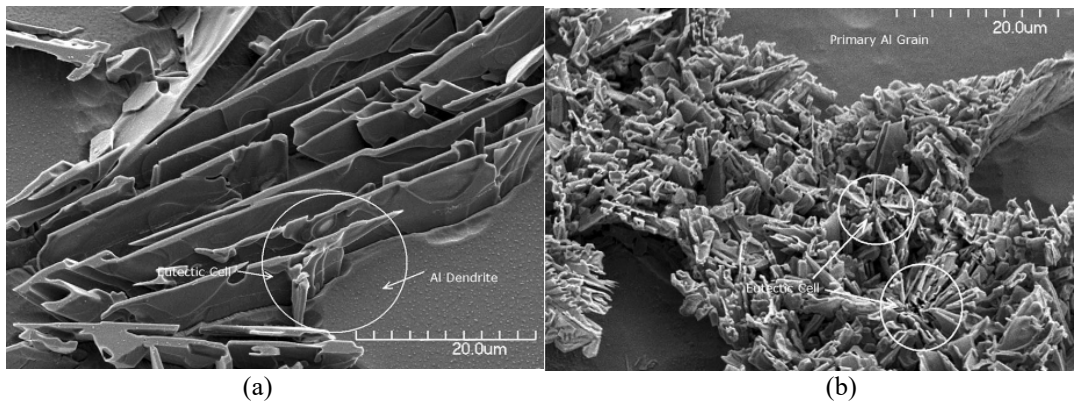


Figure 30. The eutectic structure of untreated A356 (a) and the eutectic structure of UST grain refined A356 (b).³⁵

Table 3. UTS, Yield Stress & Elongation Values of Brass Samples Produced via Different Refining Techniques³⁶

Refinement technique	UTS (MPa)	Yield Stress (MPa)	Elongation (%)
Not refined	282 (± 30)	178 (± 14)	4.3 (± 1.0)
Chemical refinement	310 (± 15)	181 (± 11)	5.0 (± 0.7)
Ultrasonic refinement at 900 °C	345 (± 15)	183 (± 10)	6.9 (± 0.5)
Ultrasonic refinement at 920 °C	367 (± 12)	187 (± 7)	9.4 (± 0.6)
Ultrasonic refinement at 940 °C	386 (± 10)	192 (± 7)	11.5 (± 0.6)

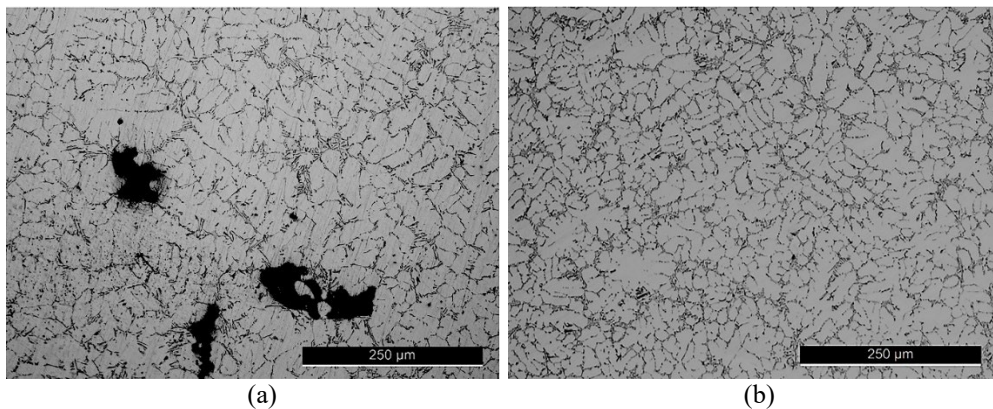


Figure 31. A microstructure of A356 untreated (a) and treated with UST in the liquid-state (b).

UST grain refinement works most efficiently at lower temperatures, below the liquidus. Figure 31 shows the effect of grain refinement when UST is applied in the liquid state at 1292F (700C). There is some evidence of refinement, however, the refinement is not as apparent as when treatment is applied in the liquid-solid state, as seen in Fig. 29.³⁵ When ultrasonic treatment is stopped before the onset of solidification, dendrites can form without any impact of streams and cavitation.

There has been evidence of grain refinement that results from ultrasonic treatment during the liquid state with some superheat, when there is no solid fraction. A study by Wang et al. suggests that any grain refinement that results from ultrasonic treatment during the liquid state is attributed to the fragmentation of oxides. During liquid state treatment, there are no solid interfaces on which cavitation and streaming can act on, however, Al_2O_3 oxides are present, which are fragmented and act as in-situ grain refiners.

In Al-0.4Ti wt% alloy, the primary intermetallic that forms are Al_3Ti . It was found that Al_3Ti intermetallics nucleate around Al_2O_3 oxide particles. Upon the application of UST in the liquid state from 1490F (810C) to 1418F (770C), the oxide clusters in the melt were broken up and homogenously dispersed via acoustic cavitation and streaming. Al_3Ti intermetallic forms around the oxide nuclei. Cavitation and streaming continue to fragment the plate-like structures, seen in Fig. 32.¹⁰ Figure 33 shows the oxide particles found at the center of unrefined and refined intermetallic compounds.¹⁰ The evidence that broken down oxide

clusters may act as internal grain refiners through liquid state UST now leads to the question, what is the minimum or maximum content of oxides that must be present for this mechanism to be successful?

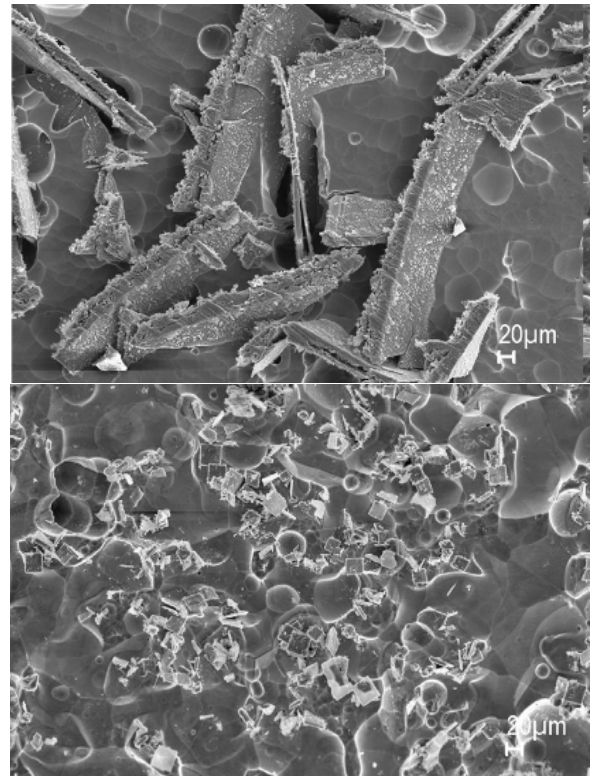


Figure 32. Al_3Ti particles without UST (top) and with UST (bottom).¹⁰

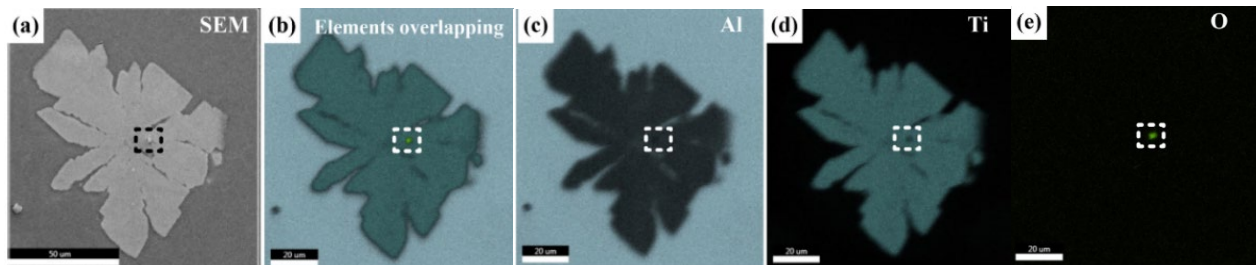


Figure 33. Characteristics of an oxide particle in the center of an Al_3Ti particle refined by UST: (a) SEM image; (b) overlapped EDS mapping image of Al, Ti and O elemental distributions; (c) EDS mapping of Al elemental distribution; (d) EDS mapping of Ti elemental distribution; (e) EDS mapping of O elemental distribution.¹⁰

SUMMARY

Ultrasonic energy imparted into the molten metal has the capability to affect and modify the resultant cast structure. Applications of ultrasonic energy for liquid metallurgical applications are still in their nascent stage; there are a vast array of applications where ultrasonic treatment of the melt can be an enabling technology. Applications vary from distributing second phase nano particles in the melt, to breaking up the oxides and causing in situ grain refinement, to modifying the intermetallics that form during the early stages of solidification.

There are three types of ultrasonic energy delivery; (i) fixed-frequency UST, (ii) fixed-frequency UST in combination with a purge gas, and (iii) variable frequency UST. Fixed-frequency UST is the most common form of treatment in literature. The goal of the combination of a fixed-frequency UST with a purge gas is to increase the survival and existence of cavitation bubbles to increase the effectiveness of treatment. Multifrequency UST focuses on system resonance to increase the effectiveness of treatment. The choice of treatment temperature is

crucial to take advantage of ultrasonic mechanisms for targeted applications.

In UST degassing, the treatment temperature should be high enough that the viscosity of the liquid metal allows for undampened treatment. In UST intermetallic morphology modification, the treatment mechanism changes with temperature from either fragmentation at a temperature where the intermetallics have already formed, or UST-assisted diffusion at a temperature where the intermetallics are about to form. Similarly in grain refinement, the mechanisms are dependent on temperature where fragmentation rules at a temperature below the liquidus.

In this work, we have reviewed the various ultrasonic delivery methods, and their effects on the resultant microstructural characteristics of the cast product. Specifically, processing parameters such as temperature, ultrasonic density per volume, and the interaction of the probe with the melt are fertile domains for further work.

ACKNOWLEDGEMENTS

The authors would like to thank Miodrag Prokic and MP Interconsulting for their valuable input and technical support. The authors would also like to thank Martijn Vos for his leadership, insight, and counsel as Chair of the ACRC focus group for this project. The authors are grateful for the support received from the industrial members of the ACRC consortium.

REFERENCES

1. Singh, S. et al., "Effect of Grain refinement, Modifier and Stirring on properties of A356," *Mater. Today Proc.* 4, 734–739 (2017).
2. Han, Y.S., "Effect of Intermetallic Phases on the Mechanical Properties of Cast A356 Alloy Wheels," *2006 International Forum on Strategic Technology* 338–341 (2006). doi:10.1109/IFOST.2006.312324.
3. Cáceres, C.H. & Selling, B.I., Casting defects and the tensile properties of an AlSiMg alloy. *Mater. Sci. Eng. A* 220, 109–116 (1996).
4. Shao, Y.W. et al., "Microstructure of As-Cast 7085 Aluminum Alloy by Homogenization," *Mater. Sci. Forum* 898, 265–271 (2017).
5. Wang, M., Xu, W. & Han, Q., "Study of Refinement and Morphology Change of AlFeSi Phase in A380 Alloy due to Addition of Ca, Sr/ Ca, Mn and Mn, Sr," *Mater. Trans.* 57, 1509–1513 (2016).
6. Eskin, G. & Eskin, D., "Ultrasonic Treatment of Light Alloy Melts (2014). doi:10.1201/b17270.
7. Sha, G. & Lissenden, C.J., "Modeling Magnetostrictive Transducers for Structural Health Monitoring: Ultrasonic Guided Wave Generation and Reception," *Sensors* 21, 7971 (2021).
8. Redwood, M., "Transient Performance of a Piezoelectric Transducer," *J. Acoust. Soc. Am.* 33, 527–536 (1961).
9. Villanueva, F., "Acoustic Impedance and Reflected Energy in Ultrasonics," (June 2, 2015). <https://www.linkedin.com/pulse/acoustic-impedance-reflectivity-ultrasonics-fernando-villanueva/> (Link last accessed 01-23-24.)
10. Wang, F. et al., "A refining mechanism of primary Al3Ti intermetallic particles by ultrasonic treatment in the liquid state," *Acta Mater.*, 116, 354–363 (2016).
11. Todaro, C.J. et al., "The Effect of Ultrasonic Melt Treatment on Macro-Segregation and Peritectic Transformation in an Al-19Si-4Fe Alloy," *Metall. Mater. Trans. A*, 48, 5579–5590 (2017).
12. Puga, H., Barbosa, J., Carneiro, V.H., Barbosa, F.V. & Teixeira, J.C., "Optimizing high-volume ultrasonic melt degassing using synchronized kinematic translation," *J. Mater. Res. Technol.*, 14, 2832–2844 (2021).
13. Friel, R.J., "Power ultrasonics for additive manufacturing and consolidating of materials," *Power Ultrasonics*, Woodhead Publishing, 313-335 (2015). |doi:10.1016/B978-1-78242-028-6.00013-2.
14. Puga, H., Tohidi, S. D., Carneiro, V.H., Meireles, J. & Prokic, M., "Ceramic Sonotrodes for Light Alloy Melt Treatment," *Int. J. Met.*, 15, 459–469 (2021).
15. "What are Sialon Ceramics?" *International Sialons* (2018). <https://www.sialons.com/resources/articles-and-guides/sialons/> (Link last accessed 01-23-24.)
16. Feng, H., Barbosa-Canovas, G. & Weiss, J., *Ultrasound Technologies for Food and Bioprocessing*. vol. 2 (2011).
17. "SCR Develops State of the Art Ultrasonic Degasser," Southwire. <https://www.southwire.com/newsroom/archive/scr-develops-state-of-the-art-ultrasonic-dtm-degasser> (Link last accessed 01-23-24.)
18. M. Prokic, MMM Ultrasonic Treatment (2001).
19. Wang, S., Kang, J., Zhang, X. & Guo, Z., "A Study on the Effect of Ultrasonic Treatment on the Microstructure of Sn-30 wt.% Bi Alloy," *Materials*, 11, 1870 (2018).
20. Jolly, M., "Prof. John Campbell's ten rules for making reliable castings," *JOM J. Miner. Met. Mater. Soc.*, 57, 19–28 (2005).
21. Talbot, D.E.J., "Effects of Hydrogen in Aluminium, Magnesium, Copper, and Their Alloys," *Int. Metall. Rev.*, 20, 166–184 (1975).
22. Sigworth, G., Williams, E. & Chesonis, D., "Gas Fluxing of Molten Aluminum: An Overview," *Essent. Read. Light Met.*, 3, 65–70 (2013).
23. Warke, V. & Makhlof, M., "Hydrogen removal from molten metal mathematical modeling and

- computer simulations," *Model. Cast. Weld. Adv. Solidif. Process.* - XI, 2, 1097–1104 (2006).
24. Shabestari, S.G., Mokarian, P. & Saeidinia, S., "Effect of process variables in rotary degassing of aluminum," *CIM Bull.*, 97, (2004).
 25. Rundquist, V., Paci, M. & von Gal, R., "The Development of an Ultrasonic Degassing Process for Aluminium Casting," *Mater. Today Proc.*, 10, 288–295 (2019).
 26. Meek, T.T., Han, Q. & Xu, H., "Degassing of Aluminum Alloys Using Ultrasonic Vibration," (2006-06-01).ORNL/TM-2006/61, 886703 <http://www.osti.gov/servlets/purl/886703-ohkArs/> (2006) doi:10.2172/886703. (Link last accessed 01-23-24.)
 27. Taylor, J.A., "Iron-Containing Intermetallic Phases in Al-Si Based Casting Alloys," *Procedia Mater. Sci.*, 1, 19–33 (2012).
 28. Lin, C., Wu, S., Zhong, G., Wan, L. & An, P., "Effect of ultrasonic vibration on Fe-containing intermetallic compounds of hypereutectic Al–Si alloys with high Fe content," *Trans. Nonferrous Met. Soc. China*, 23, 1245–1252 (2013).
 29. Cinkilic, E., Moodispaw, M., Zhang, J., Miao, J. & Luo, A.A., "A New Recycled Al–Si–Mg Alloy for Sustainable Structural Die Casting Applications," *Metall. Mater. Trans. A*, 53, 2861–2873 (2022).
 30. Barbosa, J., Puga, H., Oliveira, J., Ribeiro, S. & Prokic, M., "Physical modification of intermetallic phases in Al–Si–Cu alloys," *Mater. Chem. Phys.*, 148, 1163–1170 (2014).
 31. Cinkilic, E., Ridgeway, C.D., Yan, X. & Luo, A.A., "A Formation Map of Iron-Containing Intermetallic Phases in Recycled Cast Aluminum Alloys," *Metall. Mater. Trans. A*, 50, 5945–5956 (2019).
 32. Liu, G., Karim, M., Wang, S., Eskin, D. & McKay, B., "Processing of SiC nano-reinforced AlSi9Cu3 composites by stir mixing, ultrasonication and high pressure die casting," *J. Mater. Res. Technol.*, 18, 2384–2398 (2022).
 33. Li, H.-T., Wang, Y. & Xia, M., "Effect of intensive melt shearing on the formation of Fe-containing intermetallics in LM24 Al-alloy," *Iop Conf. Ser. Mater. Sci. Eng.* 27, (2012).
 34. Yu, L., Liu, X., Wang, Z. & Bian, X., "Grain refinement of A356 alloy by AlTiC/AlTiB master alloys," *J. Mater. Sci.*, 40, 3865–3867 (2005).
 35. Han, Q., "Ultrasonic Processing of Materials," *Metall. Mater. Trans. B*, 46, 1603–1614 (2015).
 36. Puga, H., Barbosa, J., Machado, J.M. & Vilarinho, C., "Ultrasonic grain refinement of die cast copper alloys," *J. Mater. Process. Technol.*, 263, 336–342 (2019).